

# Domino model in geodynamo

P. Hejda<sup>a</sup>, M. Reshetnyak<sup>\*,b</sup>

<sup>a</sup>*Institute of Geophysics, Academy of Sciences, 141 31 Prague, Czech Republic*

<sup>b</sup>*Institute of the Physics of the Earth, Russian Acad. Sci, 123995 Moscow, Russia*

---

## Abstract

Using Lagrangian formalism we consider evolution of the ensemble of interacting magnetohydrodynamic cyclones governed with Langevin type equations in the rotating medium. This problem is relevant to the planetary cores where the Rossby numbers are small and geostrophic balance takes place. We show that variations of the heat flux at the outer boundary of the spherical shell modulates frequency of the reversals of the mean magnetic field that is in accordance with the 3D dynamo simulations. Two scenarios of reversals were observed. Either the axial dipole decreases in favour of quadrupole and then grows in opposite direction or the mean dipole tilts and reverses without decrease of its amplitude.

*Key words:* liquid core, geomagnetic field reversals, anisotropic heat flux, thermal traps

*PACS:* 91.25.Cw

*2000 MSC:* 76F65

---

\*Corresponding author

*Email addresses:* [ph@ig.cas.cz](mailto:ph@ig.cas.cz) (P. Hejda), [m.reshetnyak@gmail.com](mailto:m.reshetnyak@gmail.com) (M. Reshetnyak)

## 1. Introduction

The present geodynamo models include thermal and compositional convection which supply the energy to the magnetic field generation in the rapidly rotating spherical shells (Olson, 2007). Due to the strong non-linearity of the system and its three-dimensionality the most reliable way of study was the numerical simulations. Because of the difference of the convective and magnetic typical times in order of magnitudes (Hollerbach, 2003) simulation of the geomagnetic field evolution is a very difficult and time consuming problem even for the modern supercomputers. The analysis of the obtained bulk of data is also very tricky process. This is motivation for considering simpler models, which can demonstrate some properties of the 3D models and present statistics for a longer time periods where the complex models fail. This way helps not only to summarise some already known results but also to predict directions of the 3D modeling, which has to deal with response of the model on various interconnected parameters.

The choice of such a model should be based on the modern knowledge of the dynamo process in the core and be proved by the observations. The specifics of the planetary convection is presence of the geostrophic state, when the scales along the axis of rotation are much larger than the scales in the perpendicular planes. The corresponding anisotropy also takes place in the wave-space and leads to the inverse cascades even for the pure hydrodynamics (Hejda and Reshetnyak, 2009). The elongated along the axis of rotation primitive convective cells are cyclones (anti-cyclones), in which the flowing up (down) liquid rotates in such a way, that helicity of the cell is negative in the northern hemisphere and positive in the southern hemisphere. This

set of cells produces the mean magnetic field at the surface of the planet, so that the cellular structure of the magnetic field is already smoothed and the dipole configuration dominates. This very simple and naive approach was successfully tested in Nakamichi et al. (2012) where the net magnetic field was produced by the ensemble of the primitive spins located at the circle at the equatorial plane. The spins rotate in the vertical plane, interact with each other and "feel" direction of the planet rotation. The energy is injected to the system with the random force which mimics buoyancy sources. Such a system produces quite reasonable sequences of the mean magnetic field reversals and can be adopted to the regimes with the variable frequency of the reversals. Here we want to extend this model, so that the spins could rotate in the horizontal plane as well. Transition to rotation of the spins in the space makes possible to describe precession of the spins around the vertical axis and, as a result, to mimic the magnetic pole wandering between the reversals and the fine structure of the reversal itself. In fact, we observe two different classes of reversals, when the spins are synchronized in the horizontal plane during the reversal or not. The first class correspond to the stable dipole field during the reversal and the second to the decaying field. The other point is influence of the external fields on the system. Here we introduce analysis of the heat-flux modulation of the frequency reversals and compare our results with the 3D dynamo simulations. We also consider how the core-mantle heterogeneity of the heat-flux can produce the preferred meridional band of the magnetic pole migration during the reversal.

## 2. Two-dimensional approach

We briefly repeat results of Nakamichi et al. (2012), which is an extension of the Ising-Heisenberg XY-models of interacting magnetic spins. For more details of the history of the problem and classification refer to Stanley (1971). The main idea of the domino model is to consider a system of  $N$  interacting spins  $\mathbf{S}_i$ ,  $i = 1 \dots N$ , in media rotating with angular velocity  $\boldsymbol{\Omega} = (0, 1)$  in the Cartesian system of coordinates  $(x, y)$ . The spins are located over an equatorial ring, are of unit length and can vary angle  $\theta$  from the axis of rotation in the range of  $[0, 2\pi]$  on time  $t$ , so that  $\mathbf{S}_i = (\sin \theta_i, \cos \theta_i)$ . Each spin  $\mathbf{S}_i$  is forced by a random force, effective friction, as well as by the closest neighboring spins  $\mathbf{S}_{i-1}$  and  $\mathbf{S}_{i+1}$ .

Following Nakamichi et al. (2012), we introduce kinetic  $K$  and potential  $U$  energies of the system:

$$\begin{aligned}
 K(t) &= \frac{1}{2} \sum_{i=1}^N \dot{\theta}_i^2, \\
 U(t) &= \gamma \sum_{i=1}^N (\boldsymbol{\Omega} \cdot \mathbf{S}_i)^2 + \lambda \sum_{n=1}^N (\mathbf{S}_i \cdot \mathbf{S}_{i+1}).
 \end{aligned}
 \tag{1}$$

The Lagrangian of the system then takes the form  $\mathcal{L} = K - U$ . Making the transition to the Lagrange equations, adding friction proportional to  $\dot{\theta}$  and the random force  $\chi$ ,

$$\frac{\partial}{\partial t} \frac{\partial \mathcal{L}}{\partial \dot{\theta}} = \frac{\partial \mathcal{L}}{\partial \theta} - \kappa \dot{\theta} + \frac{\epsilon \chi}{\sqrt{\tau}},
 \tag{2}$$

leads to the system of Langevin-type equations:

$$\begin{aligned} \ddot{\theta}_i - 2\gamma \cos \theta_i \sin \theta_i + \lambda \left[ \cos \theta_i \left( \sin \theta_{i-1} + \sin \theta_{i+1} \right) - \right. \\ \left. \sin \theta_i \left( \cos \theta_{i-1} + \cos \theta_{i+1} \right) \right] + \kappa \dot{\theta}_i + \frac{\epsilon \chi_i}{\sqrt{\tau}} = 0, \end{aligned} \quad (3)$$

$$\theta_0 = \theta_N, \theta_{N+1} = \theta_1, i = 1 \dots N,$$

where  $\gamma$ ,  $\lambda$ ,  $\kappa$ ,  $\epsilon$ ,  $\tau$  are constants. The measure of synchronization of the spins along the axis of rotation

$$M(t) = \frac{1}{N} \sum_{i=1}^N \cos \theta_i(t) \quad (4)$$

will be considered to be the total axial magnetic moment.

With the appropriate choice of parameters the simulated sequences of  $M(t)$  resembles paleomagnetic records of the magnetic dipole evolution (Nakamichi et al., 2012), and possess some important properties of the geomagnetic field: has irregular time intervals between the reversals, exhibits short drops and recoveries of the field (the so-called excursions of the magnetic field), the reconstructed 3D magnetic field, based on idea that each spin is a magnetic dipole, has similar structure as the observable one.

### 3. Three-dimensional spin model

The natural next step is generalisation of the model to the 3D spins rotation. This extension helps to dispose one of the critical disadvantages of the two-dimensional model. It is obvious, that nutation displacements in  $\theta$ -direction should cause response of the Coriolis force perpendicular to  $\theta$ - and  $\Omega$ -directions. The Coriolis force causes precession of the spins around the axis

of rotation  $\mathbf{\Omega}$  in the horizontal plane, like it happens for the magnetic spins in presence of the external magnetic field or for the spinning top. Formally this effect leads to the new evolution equation for the azimuthal angle  $\varphi$ . Below we consider how we can take into account this effect and compare it to the known equations of the rotating bodies and magnetic spins.

### 3.1. Precession and Landau-Lifshitz-Gilbert equation

In three dimensions direction of the spin  $\mathbf{S}_i = (\sin \theta_i \cos \varphi_i, \sin \theta_i \sin \varphi_i, \cos \theta_i)$  is defined by two angles in the local spherical system of coordinates. As before we suppose that origins of the coordinates are located equidistantly at the circle of the unity radius at the horizontal plane perpendicular to  $\mathbf{\Omega}$ . All the systems are obtained by translation in space, so that all corresponding axis are parallel.

First consider approximation when terms with  $\ddot{\theta}$ ,  $\ddot{\varphi}$  and quadratic in  $\dot{\theta}$   $\dot{\varphi}$  are neglected. Then, using that fact that for the precession-like solution the term proportional to  $\dot{\varphi} \cos \theta$  should be included in the Lagrangian (Miltat et al., 2002), this leads to the  $i^{th}$  spin

$$\mathcal{L}_i = \dot{\varphi}_i \cos \theta_i - \gamma (\mathbf{\Omega} \cdot \mathbf{S}_i)^m - \mathcal{I}_i, \quad (5)$$

where  $m$  is integer. The interaction term can be written as follows:

$$\begin{aligned} \mathcal{I}_i &= \lambda [(\mathbf{S}_i \cdot \mathbf{S}_{i+1}) + (\mathbf{S}_i \cdot \mathbf{S}_{i-1})] = \\ &\lambda \left[ \sin \theta_i (\sin \theta_{i+1} \cos(\varphi_i - \varphi_{i+1}) + \sin \theta_{i-1} \cos(\varphi_i - \varphi_{i-1})) + \right. \\ &\quad \left. \cos \theta_i (\cos \theta_{i+1} + \cos \theta_{i-1}) \right]. \end{aligned} \quad (6)$$

Further we consider two cases: i)  $m = 1$  corresponds to ferromagnetics,

when direction of the external magnetic field is important and the spins are co-directional to  $\mathbf{\Omega}$ ; ii) for  $m = 2$  the both directions  $\pm\mathbf{\Omega}$  are equivalent, so that the potential energy concerned with rotation is symmetric relative to the equatorial plane as it was assumed in 2D case (3). As according to the paleomagnetic observations there is no preferable polarity of the magnetic field and the Lorentz force in MHD equations is quadratic on the magnetic field, the latter case is more suitable for our tasks. As we see below the first two terms in r.h.s. of (5) for  $m = 1$  leads to Landau-Lifshitz-Gilbert (LLG) equation, which describes precession of the magnetic spin in the non-dissipative medium in the external Zeeman magnetic field equal to  $\mathbf{\Omega}$ . The third term describes local interactions of the spins. Now we write the Lagrange equations for 4 independent variables  $(\theta, \varphi, \dot{\theta}, \dot{\varphi})$ :

$$\begin{aligned} \frac{d}{dt} \frac{\partial \mathcal{L}}{\partial \dot{\theta}_i} - \frac{\partial \mathcal{L}}{\partial \theta_i} + \frac{\partial \mathcal{F}}{\partial \dot{\theta}_i} + \frac{\partial \mathcal{R}_i}{\partial \theta} &= 0, \\ \frac{d}{dt} \frac{\partial \mathcal{L}}{\partial \dot{\varphi}_i} - \frac{\partial \mathcal{L}}{\partial \varphi_i} + \frac{\partial \mathcal{F}}{\partial \dot{\varphi}_i} + \frac{\partial \mathcal{R}_i}{\partial \varphi_i} &= 0, \end{aligned} \tag{7}$$

where

$$\mathcal{F}_i = \frac{\kappa}{2} \left( \dot{\theta}_i^2 + \sin^2 \theta_i \dot{\varphi}_i^2 \right), \quad \mathcal{R}_i = \frac{\epsilon}{\sqrt{\tau}} (\theta_i \chi_i + \varphi_i \psi_i), \tag{8}$$

and  $\psi$  is the random function.

Substitution of (5) and (8) in (7) for  $m = 2$ , leads to the following system

of equations:

$$\begin{aligned} \dot{\theta}_i - \kappa \sin \theta_i \dot{\varphi}_i - \frac{\mathcal{I}'_{i\varphi}}{\sin \theta_i} - \frac{\epsilon \psi_i}{\sin \theta_i \sqrt{\tau}} &= 0, \\ \dot{\varphi}_i + \kappa \frac{\dot{\theta}_i}{\sin \theta_i} - 2\gamma \cos \theta_i + \frac{\mathcal{I}'_{i\theta}}{\sin \theta_i} + \frac{\epsilon \chi_i}{\sin \theta_i \sqrt{\tau}} &= 0. \end{aligned} \quad (9)$$

The exact form of the terms with derivatives of  $\mathcal{I}_i$  are given by equations:

$$\begin{aligned} -\frac{\mathcal{I}'_{i\varphi}}{\sin \theta_i} &= \lambda \left[ \sin \theta_{i+1} \sin(\varphi_i - \varphi_{i+1}) + \sin \theta_{i-1} \sin(\varphi_i - \varphi_{i-1}) \right], \\ \frac{\mathcal{I}'_{i\theta}}{\sin \theta_i} &= \lambda \left[ \cot \theta_i \left( \sin \theta_{i+1} \cos(\varphi_i - \varphi_{i+1}) + \sin \theta_{i-1} \cos(\varphi_i - \varphi_{i-1}) \right) - \right. \\ &\quad \left. \left( \cos \theta_{i+1} + \cos \theta_{i-1} \right) \right]. \end{aligned} \quad (10)$$

Like before in 2D case (3), we use the periodical boundary conditions:

$$\theta_0 = \theta_N, \theta_{N+1} = \theta_1, \varphi_0 = \varphi_N, \varphi_{N+1} = \varphi_1, i = 1 \dots N. \quad (11)$$

Since Lagrangian (5) does not include quadratic terms proportional to  $\dot{\theta}^2$ ,  $\dot{\varphi}^2$ , equations (9) present balance of the forces. Before we come to analysis of the system (9), we consider case  $m = 1$ , where the term with  $2\gamma \cos \theta$  in (9) changes to  $\gamma$ . Putting  $\lambda = 0$ ,  $\kappa = 0$ ,  $\epsilon = 0$ , yields  $\dot{\theta} = 0$ ,  $\dot{\varphi} = \gamma$ , i.e. precession around axis  $z$ , that corresponds to the solution of the LLG equation without dissipation for ferromagnetics:

$$\dot{\mathbf{S}}_i = -\gamma \mathbf{S}_i \times \boldsymbol{\Omega}, \quad (12)$$



which has integral of motion  $\frac{\partial}{\partial t} \mathbf{S}_i^2 = 0$ , and for the constant in time  $\mathbf{\Omega}$  the other integral:  $\frac{\partial}{\partial t} (\mathbf{S}_i \cdot \mathbf{\Omega}) = 0$ , that follows to  $\dot{\theta} = 0$ . The  $x$ -component of equation (12) gives the already mentioned above equation for the azimuthal angle:  $\dot{\varphi} = \gamma$ . Existence of precession distinguishes the 3D case from 2D, where the role of rotation comes to attraction of the spins to the poles. (3), so that derivative  $\frac{\partial \mathcal{L}}{\partial \theta}$  moves from  $\theta$ -component equation to  $\varphi$ -equation.

For the case  $m = 2$  one gets precession-like equation  $\dot{\theta} = 0$ ,  $\dot{\varphi} = 2\gamma \cos \theta$ , which predicts reversal of the angular velocity of the spins at the equator plane. Obvious, that due to the distinguished direction concerned with rotation the whole system is not symmetric to the change of  $z \rightarrow -z$  and the break of the reflection symmetry for  $m = 1$  gives preferable polarity of the magnetic field ( $\overline{\sin \theta} \neq 0$ ). For  $m = 2$  one has  $\overline{\sin \theta} \rightarrow 0$ , however  $\dot{\varphi}$  changes its sign at the equatorial plane  $z = 0$ . Below we consider this phenomenon in more details.

It is instructive to consider balance of the curvilinear terms and the Coriolis force in  $V_\theta$ - and  $V_\varphi$ -components of the Navier-Stokes equation in the spherical system of coordinates with  $V_r = 0$ :

$$-V_\varphi^2 \cot \theta = H V_\varphi \cos \theta, \quad V_\theta V_\varphi \cot \theta = -H V_\theta \cos \theta, \quad (13)$$

where  $H$  is the amplitude of the Coriolis force, and tangential velocity ( $V_\theta, V_\varphi$ ) is  $(\dot{\theta}, \dot{\varphi} \sin \theta)$ . The both equations in (13) gives  $\dot{\varphi} = -H$ , that corresponds to the case with  $m = 1$  and  $V_\theta$  remains undefined. As we see, condition of equiprobability of the direct and inverse polarity for  $m = 2$  changes the whole scenario.

Return to (9) with  $m = 2$ . Since we have omitted quadratic in velocities terms, this approximation is valid for the slow regimes with precession between the reversals of the field. Anyway we consider how the predicted asymmetry of the precession velocity is influenced by the random force. Even for the small random force distribution of  $V_\varphi(M)$  in Fig.1a for the regime without reversals in Fig.1b has zero mean value. The reason of such a seeming discrepancy with our estimate  $\dot{\varphi} \sim \cos \theta$  is the following. Consider averaged in time coupled equations (9) in the simplified form without interaction, diffusion and random forces for small  $\theta \ll 1$  and constant in time between the reversals of the magnetic field  $\bar{\theta} = 0$  and check if  $\dot{\varphi}$  still changes sign for the coupled system:  $\bar{\theta} \sim \overline{\theta \dot{\varphi}} = 0$ ,  $\overline{\theta \dot{\varphi}} + \bar{\theta} \sim \gamma \overline{(1 - \theta^2) \theta}$  that leads to the contradiction:  $\overline{\theta \dot{\varphi}} \sim \gamma \bar{\theta} \neq 0$ , that means that the other terms should be included in the consideration and naive prediction of change of the sign for  $\dot{\varphi}$  is wrong. We conclude, that the random forcing makes system symmetric to the change of  $\varphi$ -direction. Here we do not consider extremely small  $\epsilon$  regimes to preserve the realistic for the geomagnetic field level of the field fluctuations between the reversals.

The considered approximation with the small fluctuations of  $\theta$  is reliable for some astronomical problems without nutation, as well as to the ferromagnetic problems when the temperature is less than the Curie point and  $\theta$ -variations are small. This review was used from the methodological point of view and now we come to the full equations applicable to the highly non-linear regimes with the large accelerations.

### 3.2. Precession and nutations

Now we consider approximation with large  $\ddot{\theta}$ ,  $\ddot{\varphi}$ ,  $\dot{\theta}^2$ ,  $\dot{\varphi}^2$  using analogy to the spinning top with unity moments of inertia (Landau and Lifshitz, 2005) with Lagrangian in the form:

$$\mathcal{L}_i = \frac{1}{2} \left( \dot{\theta}_i^2 + \sin^2 \theta_i \dot{\varphi}_i^2 + (\dot{\varphi}_i \cos \theta_i + \dot{\zeta}_i)^2 \right) - \gamma (\mathbf{\Omega} \cdot \mathbf{S}_i)^2 - \mathcal{I}_i + \Psi_i, \quad (14)$$

where  $\dot{\zeta}_i$  is angular velocity of the top. In our case  $\dot{\zeta}$  is fixed and given property of the spin. For simplicity we take it equal to unity:  $\dot{\zeta}_i^2 \equiv |\mathbf{S}_i|^2 = 1$ . The new variable  $\Psi$  is the potential used latter for description of the external forces.

Finally Lagrangian can be written as follows

$$\mathcal{L}_i = \frac{1}{2} \dot{\theta}_i^2 + \frac{1}{2} \dot{\varphi}_i^2 + \dot{\varphi}_i \cos \theta_i - \gamma \cos^2 \theta_i - \mathcal{I}_i + \Psi_i, \quad (15)$$

where constant is omitted because Lagrange equations includes only derivatives of  $\mathcal{L}$ . Neglecting of the quadratic terms in velocities in (15) leads to the simplified version of Lagrangian (5).

Substitution of (14) in (7) yields to the dynamic equations:

$$\begin{aligned} \ddot{\theta}_i + \dot{\varphi}_i \sin \theta_i - \gamma \sin 2\theta_i + \mathcal{I}'_{i\theta} + \kappa \dot{\theta}_i + \frac{\epsilon \chi_i}{\sqrt{\mathcal{T}}} - \Psi'_{i\theta} &= 0, \\ \ddot{\varphi}_i - \sin \theta_i \dot{\theta}_i + \mathcal{I}'_{i\varphi} + \kappa \sin^2 \theta_i \dot{\varphi}_i + \frac{\epsilon \psi_i}{\sqrt{\mathcal{T}}} - \Psi'_{i\varphi} &= 0. \end{aligned} \quad (16)$$

Neglecting the second in time derivatives and quadratic terms leads to the original system (9).

Note, that in contrast to 2D case we already have two equations, that

requires "energy" balance fulfilment, and the new numerical methods should be used. This point is enforced by that fact, that there are terms with  $\sin \theta$  in the denominator. That was the reason to use Newton-Raphson iterative method in the residual form described in the Appendix.

Now we consider important for the geomagnetism question on the predictability of the geomagnetic field reversal on the secular variations before the reversal (Jacobs, 2005) and take as a measure of variations the amplitude of the magnetic dipole precession velocity  $V_\varphi$  around the geographical pole. Using equations (16) we generate 30 reversals of the field, see Fig.2(1). Taking the typical time  $t_i$  between the reversals as  $3 \cdot 10^5$ y we come to the estimate of the full time interval as  $9 \cdot 10^6$ y and the time unity  $\tau_u = 3 \cdot 10^5 / 2 \cdot 10^4 = 4 \cdot 500$ y. The estimate of the azimuthal velocity  $V_\varphi = 0.2$  leads in the order of magnitude to the typical archeomagnetic time estimate of the pole wandering (similar to the west drift velocity)  $\tau_a = \frac{\pi}{8} \frac{1}{V_\varphi} \tau_u \sim 3 \cdot 500$ y, where we took into account, that between the reversals the pole locates in the cone  $\theta < \frac{\pi}{8}$ .

We inspect the set of the five reversals of the magnetic field, see Fig.2(2). The particular feature of this regime is existence of the intermediate state corresponding to the small  $|M|$  when the system does not know in what direction it should go, and as a result some of the reversals fails producing excursions, see Fig.2(1). To check possibility of the reversal predictability we consider the mean values of  $\overline{M}$  and  $|\overline{V_\varphi}|$  over these five reversals, see Fig.2(3, 4). As we see, the change of polarity does not lead to the substantial change of  $|\overline{V_\varphi}|$ , that means that the behaviour of the model is symmetric in respect to the moment of the reversal.

#### 4. Magnetic field of the spins

The essential disadvantage of the domino model based on the assumption of the long-range interactions for the spins is absence of connection between the spin's position and its magnetic field. That was the reason why we still used integral characteristic  $M$  as a measure of the field. Let us summarise requirements to the model which we want to satisfy: i) the potential energy of the spins should have minimum when they are located near the poles and the spins should have the same direction; ii) the model provides calculation of 3D magnetic field at least at some distance from the spins. Identification of the spins with the magnetic dipoles helped Nakamichi et al. (2012) to get 3D distribution of the magnetic field for the spins in the form:

$$\mathbf{B} = \frac{3 \mathbf{r} (\mathbf{d} \cdot \mathbf{r}) - r^2 \mathbf{d}}{r^5}, \quad (17)$$

where  $\mathbf{d}$  is a magnetic moment of the dipole in the centre of the coordinates and  $\mathbf{r}$  is the radius-vector of observation. It should be noted, that as follows from (17), the stable state of two magnetic dipoles at the distance  $R$  with corresponding potential energy of interaction

$$U = \frac{3 (\mathbf{d}_1 \cdot \mathbf{R})(\mathbf{d}_2 \cdot \mathbf{R}) - (\mathbf{d}_1 \cdot \mathbf{d}_2) R^2}{R^5} \quad (18)$$

is quadrupole, when the magnetic moments  $\mathbf{d}_1$ ,  $\mathbf{d}_2$  are anti-parallel. In its turn this would correspond to the death of the dipole magnetic field at large  $R$  and relation (18) is out of interest for geomagnetism.

To overcome this problem and to get the self-organised mean dipole field Nakamichi et al. (2012) suggested to use the simplified version of (18) with

omitted first term and opposite sign for the second term, see (1). This form is similar to that one in the ferromagnetics where magnetic domains enforce the external magnetic field choosing the same with it direction. In ferromagnetics this effect has the pure quantum origin concerned with the exchange energy of the magnetic domains. As regards to (Nakamichi et al., 2012) it was just postulated as a convenient way to get similar to observations results and we join this idea in the rest of the paper.

Using equation (17) for the set of  $N$  magnetic dipoles, located at the circle of unity radius we compute the vector magnetic field, see distribution of its radial component at the distance of the three unity length  $\mathcal{R}$  during one of the reversal in Fig.3. One of the specific features of this reversal is existence of the preferred meridional band where the reversal occurs, see Fig.3(2). To consider this effect in more details we come to analysis of the spectral properties, see evolution of the axial dipole Gauss coefficient  $g_1^0$ , in Fig.4(1), at the distance  $\mathcal{R}$  for the five reversals in Fig.2(1). We conclude that the typical time of the drop and recover of the field during the reversal in this model is the same, there is some increases of the field just before and after the reversal. So as the amplitude of the spins is fixed the net magnetic flux of  $|\mathbf{B}|$  is constant in time as well as its spectrum, during, e.g., the reversal. This leads to the exchange of the magnetic energy between the dipole and quadrupole modes in Fig.4(2), where the ratio of the dipole and quadrupole modes gives  $\overline{\mathcal{D}}/\overline{\mathcal{Q}} \approx 13$  compared in order of magnitudes with that at the surface of the Earth. In the moment of the reversal  $t \sim 2\,100 \mathcal{D}$  drops, and intensity of the quadrupole  $\mathcal{Q}$  increases to the level of the dipole field. This effect is known in 3D simulations as well. The reason of such a distribution

is that magnetic energy in the geostrophic systems is quite large and hardly can be immediately transferred to the kinetic energy during the reversal. It means that the drop of the dipole field should be compensated with increase of the higher modes.

The other, may be the more specific feature of the domino model is that for the other four reversals the amplitude of the total dipole field during reversal is constant. In contrast to the previous case, where due to the uncorrelated horizontal projections of the dipole field the averaged dipole field decreased, the second case corresponds to the coherent state when even during the reversal all the spins have the same direction. For this scenario the mean dipole field rotates in the meridional plane without decrease of the amplitude. As we see, this three-dimensional phenomenon for the considered regime is more expected and caused by interaction of the spins (16) in  $\varphi$ -direction during the reversal with the short interaction time compared to the times of the reversal and precession. The both scenarios does not contradict to observations.

## 5. Thermal flux heterogeneities

One of the important results of the geodynamo theory is that frequency of the reversals depend on the spatial distribution of the heat flux at the core-mantle boundary (Glatzmaier et al., 1999). Fluctuations of the heat flux of order 10–20% of the mean flux value caused with the processes in the mantle and D'' layer have typical time scales  $10^6$ - $10^7$ y, are much larger time scales in the liquid core  $10^4$ - $10^5$ y. In particular increase of the heat flux towards the poles is equivalent to increase of rotation, that damps the

reversals. Such fluctuations appears to be the thermal traps for reversals. In its turn, the decrease of the heat flux in the high latitudes leads to chaotic behaviour of the magnetic dipole and increase of the reversal frequency, when the Archimedean forces become more significant. This effect corresponds to increase of the Rossby number, which has threshold at 0.12 where regime of the stable dipole field changes to the regime of the frequent reversals. It looks tempting to reproduce this effect in the domino model, where the large number of the reversals can be easily simulated.

We now extend the concept of the spin from the purely magnetic system to the whole cyclone system, including its hydrodynamics, and we introduce correction  $\Psi(\theta, \varphi)$  to the potential energy  $U$ , which takes into account the heterogeneity of the thermal flux. The new effective force  $\mathbf{F}_i$  is proportional to the corresponding derivatives of  $\Psi_i$  with the opposite sign will appear in (16). Here we study influence of the various forms of  $\Psi$  on the behaviour of  $M(t)$ .

Let  $\Psi(t, \theta, \varphi) = C_\psi \psi(t, \theta, \varphi)$ , where  $C_\psi$  is a constant, and the spatial distribution of the potential is given by  $\psi = -\cos^2 \theta$ . Accordingly to the recent estimates of the heat-flux variations at the core-mantle boundary, which can be about 20% (Olson et al., 2002), we conclude that  $C_\psi \sim 0.2 \frac{\epsilon}{\sqrt{\tau}} \sim 1$ . Then,  $C_\psi > 0$  corresponds to the stable state in the polar regions,  $\theta = 0, \pi$ , and the appearing force  $F = -\sin 2\theta$ , acting on the cyclones, is directed towards the poles. This regime corresponds to the increase of the thermal flux near the poles that causes the stretching of the cyclone along the axis of rotation. So as  $F$  changes sign at the pole  $\theta = \pi$ , and the force is directed to the pole (or outward) for  $\theta \rightarrow \pi - 0$  and  $\theta \rightarrow \pi + 0$ , we can consider it



as the spherical coordinate when it is needed. In Fig.5 we demonstrate the effective influence of  $F$  on  $M$  for the regime in 2(1). The increase of the thermal flux along the axis of rotation leads to the partial suppression of the reversals of the field, Fig.5(1). Note that, for the chosen potential barrier  $\psi$ , the dependence of  $F$  is equal to the  $\gamma$ -term in (3): the increase of the thermal flux at the poles leads to the effective increase of rotation and amplification of geostrophy, caused by the rapid daily rotation of the planet. Our results are in agreement with the 3D simulations, see Fig.1d in (Glatzmaier et al., 1999). The further increase of  $C_\psi$  ( $C_\psi = 2$ ) leads to the total stop of the reversals. It is more interesting that, using even larger  $C_\psi > 10$ , one arrives at regimes with a nearly constant in time  $|M| \leq 1$  defined by the initial distribution of  $\mathbf{S}_i$ . In other words, the super flux at the poles can fix the spins which are still not coherent. There is some evidence (Shatsillo et al., 2005) that the geomagnetic dipole in the past could have migrated from the usual position near the geographic poles to some stable state in the middle latitudes. Within the framework of our model, we can explain this phenomenon by the thermal super flux at the poles. Later we will discuss some other scenarios which yield similar results.

For negative  $C_\psi$ , when the geostrophy breaks due to the relative intensification of convection in the equatorial plane, we get the opposite result, see Fig.5(2): the regime of the frequent reversals observed in Fig.1c in (Glatzmaier et al., 1999). In this case force  $F$  is directed from the poles and the equilibrium point at the poles becomes unstable. The new minimum of the potential energy at the equator leads to the appearance of a new attractor, with the dipole at the low latitudes. Similar behaviour of the

magnetic dipole is observed on Neptune and Uranus; for more details see, e.g. (Cupal et al., 2002).

Now we consider the non-axial-symmetrical potentials. Let  $\psi = \cos^2 \theta \cdot \cos^2 \varphi$ . It is clear to see, that for the large  $|C_\psi|$  frequency of the reversals should follow the previous axial-symmetrical case of  $\psi$ , in particular for  $C_\psi = 3$  the number of reversals decreases, see Fig.5(3). Moreover, this form of  $\psi$  with dependence on  $\varphi$  leads to the new effect: appearing of the preferred meridional band of the magnetic poles migration during the reversals. We compare distribution of  $h_1^1(g_1^1)$  without potential, see Fig.6(1), with that one with the non-axialsymmetrical potential. For the first one we have isotropic distribution of the horizontal dipoles, see Fig.6(1). Insertion of the potential leads to appearing of the barriers for the reversals with gaps at  $\varphi = 0$  and  $\varphi = \pi$ , see Fig.6(2), where the large circles corresponding to the magnetic dipole at the equator plane have the elliptical distribution, and near the poles (small circles) distributed isotropically. For the considered form of  $\psi$  sign of  $F_\theta$  did not change in  $\varphi$ .

The last example is with  $F_\theta(\varphi)$  changing sign at the equator plane:  $\psi = \cos^2 \theta \cdot \sin 2\varphi$ , see Fig.6(3), with the only one reversals for the model simulation and the anisotropy observed for all positions of the integral dipole, even for the locations near the poles, when the amplitude of horizontal dipole  $\sqrt{g_1^{12} + h_1^{12}}$  is small. In other words, fluctuations of the heat flux causes not only preferred meridional bands of the magnetic poles migration, but the anisotropy of the poles locations between the reversals as well. We also observe states, when for the large  $|C_\psi|$  reversals stop because some of the spins come to the thermal trap near the poles (for some particular values of  $\varphi$ ) and

the full reversal which includes reversals of all spins is impossible.

## 6. Conclusion

It appears, that even a small extension of the original toy domino model leads to some nice physical effects known in the various fields of physics. In spite of simplicity of this approach it has very strong advantage: one can test very different scenarios of magnetic field evolution basing on some realistic information on the cyclone convection in the core. This approach is well designed for modelling of interaction on the different scales and number of the neighbour cyclones, which can be obtained from the 3D models. The other possibility is to use two distinct sets of cyclones inside and outside of the Taylor cylinder, which separates two different regions in the liquid core.

We also believe, that domino models can be modified for the analysis of the net kinetic and may be current, magnetic helicities as well. The first kind of helicities is the most preferable for the analysis, because the cyclone's hydrodynamics to some level is stable during the reversals, what is not the case for the generated in the cyclone magnetic field. The latter obstacle makes interpretation of the results in the domino model not so unambiguous.

### A.

We rewrite system (16) in the form of the first order differential equations:

$$\begin{aligned}
 V_i - \dot{\theta}_i &= 0, \\
 W_i - \dot{\varphi}_i &= 0, \\
 \dot{V} + \kappa V + W \sin \theta_i + A &= 0, \\
 \dot{W} - \sin \theta_i V + \kappa \sin^2 \theta_i W + B &= 0,
 \end{aligned}
 \tag{19}$$

relative to the vector

$$\mathbf{y}^n = \begin{pmatrix} V^n \\ W^n \\ \theta^n \\ \varphi^n \end{pmatrix}, \quad (20)$$

where

$$A = -\gamma \sin 2\theta_i + \mathcal{I}'_{i\theta} + \frac{\epsilon \chi_i}{\sqrt{\tau}} - \Psi'_{i\theta}, \quad B = \mathcal{I}'_{i\varphi} + \frac{\epsilon \psi_i}{\sqrt{\tau}} - \frac{1}{\sin \theta_i} \Psi'_{i\varphi}. \quad (21)$$

Using the implicit first order Euler scheme in time for the  $n^{\text{th}}$  time step we introduce residual vectors for (19):

$$\mathbf{e}^n = \begin{pmatrix} V^n dt - \theta^n + \theta^{n-1} \\ W^n dt - \varphi^n + \varphi^{n-1} \\ V^n - V^{n-1} + \kappa V^n dt + W^n \sin \theta_i^n dt + A^n dt \\ W^n - W^{n-1} - \sin \theta_i^n V^n dt + \kappa \sin^2 \theta_i^n W^n dt + B^n dt \end{pmatrix}. \quad (22)$$

The iterative Newton-Raphson process for the  $p^{\text{th}}$ -iteration gives:

$$\mathbf{y}_p^n = \mathbf{y}_{p-1}^n - \left( \frac{\partial \mathbf{e}_{p-1}^n}{\partial \mathbf{y}_{p-1}^n} \right)^{-1} \cdot \mathbf{e}_{p-1}^n, \quad (23)$$

where Jacobian matrix has form:

$$\hat{j} = \frac{\partial \mathbf{e}_p^n}{\partial \mathbf{y}_p^n} = \begin{bmatrix} dt & 0 & -1 & 0 \\ 0 & dt & 0 & -1 \\ 1 + \kappa dt & \sin \theta_i^n dt & W^n \cos \theta_i^n dt + \frac{\partial A^n}{\partial \theta} dt & \frac{\partial A^n}{\partial \varphi^n} dt \\ -\sin \theta_i^n dt & 1 + \kappa \sin^2 \theta_i^n dt & J_{43} & \frac{\partial B^n}{\partial \varphi^n} dt \end{bmatrix}, \quad (24)$$

$$J_{43} = -\cos \theta_i^n V^n dt + \kappa \sin 2\theta_i^n W^n dt + \frac{\partial B^n}{\partial \theta^n} dt. \quad (25)$$

For each time moment  $n$  and spin  $i$  one has iterative process (23) with updated other spin values. After the desired convergence is reached transition to the new time step  $n+1$  is done. At the each time step we check conditions  $\theta_i \in (0, 2\pi)$ ,  $\varphi_i \in (0, 2\pi)$  and correct values if necessary. This algorithm appears to be stable to singularity at the axis and can be easily transformed to the second-order Crank-Nicolson scheme in time. Anyway this problem is more stable than the PDE in the spherical coordinates, because the large derivatives near the pole forces spins to go out from the pole region and instability in such a self-organised way is damped. The spins are squeezed from the pole regions.

## References

- Cupal, I., Hejda, P., Reshetnyak, M., 2002. Dynamo model with thermal convection and with the free-rotating inner core. *Planet. Space Sci.* 50, P.1117–1122.
- Glatzmaier, G.A., Coe, R.S., Hongre, L., Roberts, P.H., 1999. The role of

- the Earth's mantle in controlling the frequency of geomagnetic reversals. *Nature*. 401, 885–890.
- Hejda, P., Reshetnyak, M., 2009. Effects of anisotropy in the geostrophic turbulence. *Phys. Earth Planet. Int.* 177, 152–160.
- Hollerbach, R., 2003. The range of timescales on which the geodynamo operates. V. Dehant, K. Creager, S.-I. Karato & S. Zatman (Editors), *Earth's Core: Dynamics, Structure, Rotation*, AGU Geodynamics Series. 31, 181–192.
- Jacobs, J.A., 2005. *Reversals of the Earth's Magnetic Field*. Cambridge University Press, Cambridge.
- Jones, C.A., 2011. Planetary magnetic fields and fluid dynamos. *Phil. Trans. R. Soc. London.* 43, 583–614.
- Krause F., Rädler K.-H., 1980. *Mean field magnetohydrodynamics and dynamo theory*. Akademie-Verlag, Berlin.
- Landau, L.D., Lifshitz, E.M., 2002. *Mechanics*, 3rd Edition. Butterworth-Heinemann, Oxford.
- Miltat, J., Albuquerque, G., Thiaville, A., 2002. An introduction to micromagnetics in the dynamic regime. *Topics Appl. Phys.* 83, 1–34.
- Nakamichi, A., Mouri, H., Schmitt, D., Ferriz-Mas, A., Wicht, J., Morikawa, M., 2012. Coupled spin models for magnetic variation of planets and stars. *Mon. Not. R. Astron. Soc.* 423, 4, 2977–2990, arXiv:1104.5093v1.
- Olson, P.L., Coe, R.S, Driscoll, P.E., Glatzmaier, G.A, Roberts, P.H., 2010. Geodynamo reversal frequency and heterogeneous core–mantle boundary heat flow. *Phys. Earth Planet. Inter.* 180, 66–79.
- Treatise on Geophysics, V.8: Core Dynamics, Olson, P., Ed., London: Elsevier, 2007.
- Parker, E.N., 1955. Hydromagnetic Dynamo Models. *Astrophys. J.* 122, 293–314.
- Pedlosky J., 1987. *Geophysical Fluid Dynamics*. Springer-Verlag, NY.

- Rudiger, G., Hollerbach, R., 2004. *The Magnetic Universe: Geophysical and Astrophysical Dynamo Theory*. Wiley VCH, Weinheim.
- Shatsillo, A. V., Didenko, A.N. Pavlov, V.E., 2005. Two competing Paleomagnetic directions in the Late Vendian: New data for the SW Region of the Siberian Platform. *Russ. J. Earth Sci.* 7, 4, 3–24.
- Stanley, H.E., 1971. *Introduction to phase transitions and critical phenomena*. Clarendon Press, Oxford.

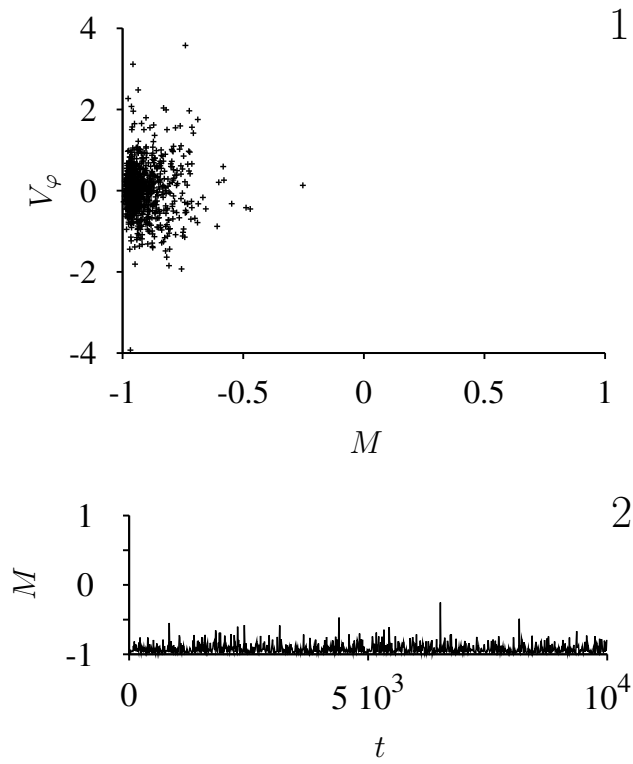


Figure 1: Dependence of velocity precession  $V_\varphi$  on dipole polarity  $M$  (1) and evolution of the dipole  $M$  in time (2) for  $\gamma = -1.8$ ,  $\lambda = -6$ ,  $\kappa = 0.1$ ,  $\epsilon = 0.03$ ,  $\tau = 0.01$ .



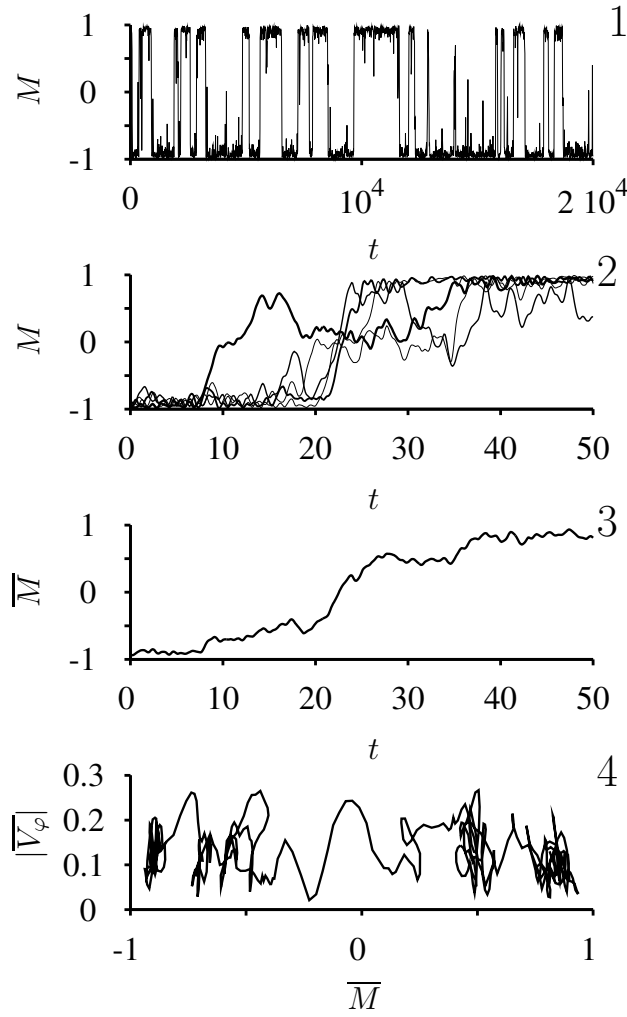


Figure 2: Evolution in time of  $M$  for  $\gamma = 1$ ,  $\lambda = -4.8$ ,  $\epsilon = 0.8$ ,  $\kappa = 0.2$  (1) and reversals of the magnetic field (on degree of thickness of the line) for 5 time intervals (9640, 9690), (12000, 12050), (12260, 12310), (17840, 17890), (18670, 18720) where for the 3rd and 5th interval sign of  $M$  is changed (2); (3) – the mean value  $\overline{M}$  for the previous plot (2) and the mean precession velocity  $|\overline{V}_\varphi|$  vice  $\overline{M}$  (4).

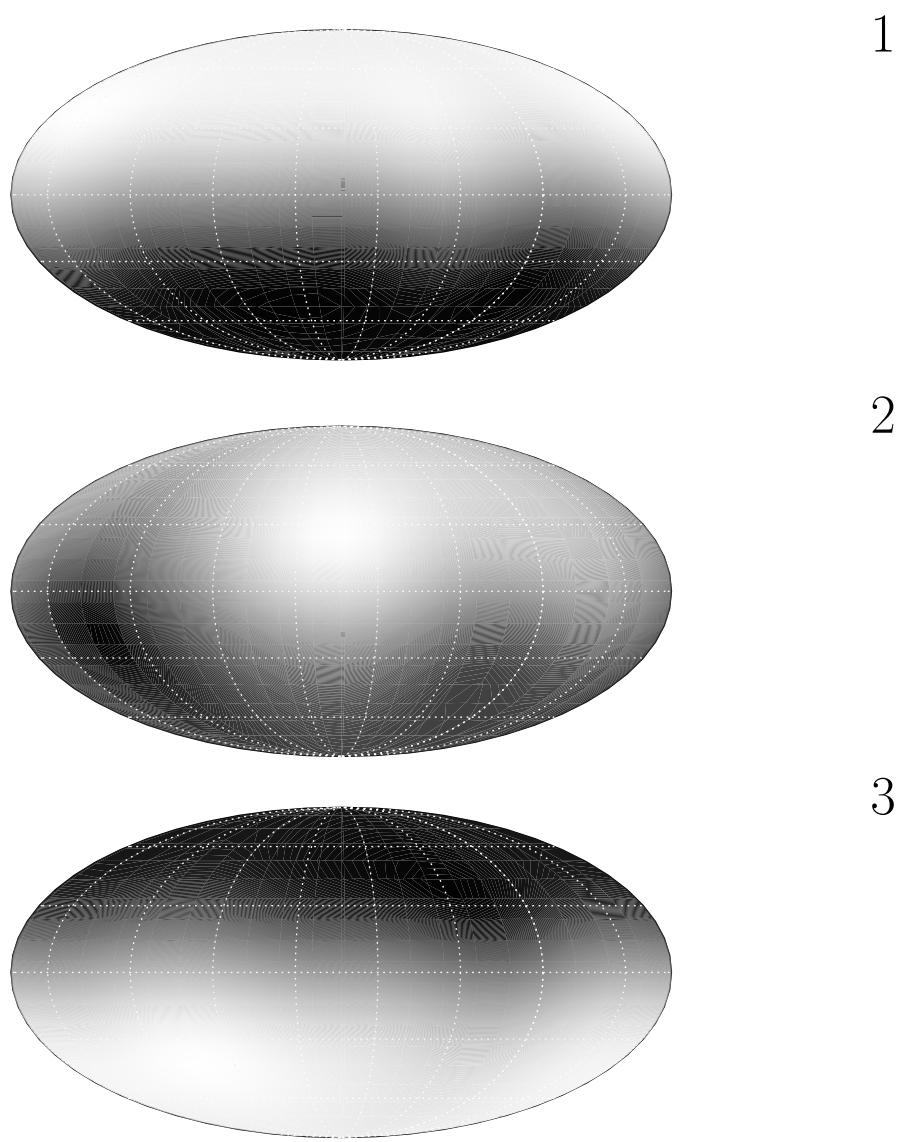


Figure 3: The map of  $B_r$ -component of the magnetic field in the Mollweide projection for the time moments  $t = 2500$  (1), 2600 (2), 2700 (3). The white colour corresponds to the positive values and the black one to the negative.

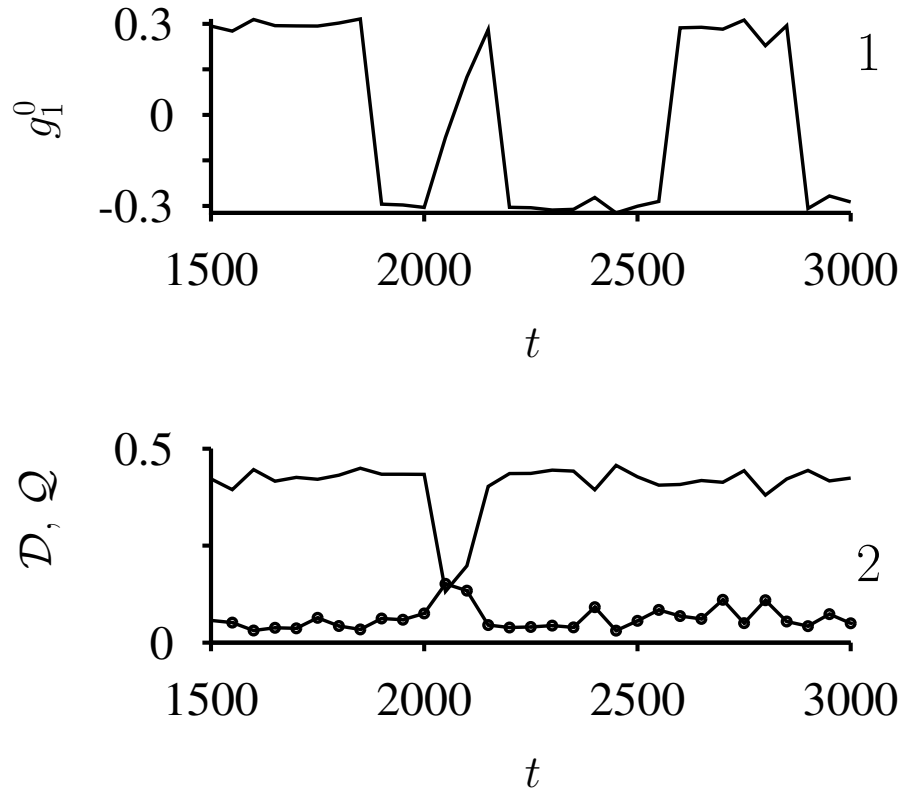


Figure 4: Evolution of  $g_1^0$  (1) and (2)  $\mathcal{D} = \sqrt{2} \sqrt{g_1^{02} + g_1^{12} + h_1^{12}}$  (solid line),  $\mathcal{Q} = \sqrt{3} \sqrt{g_2^{02} + g_2^{12} + h_2^{12} + g_2^{22} + h_2^{22}}$  (circles).

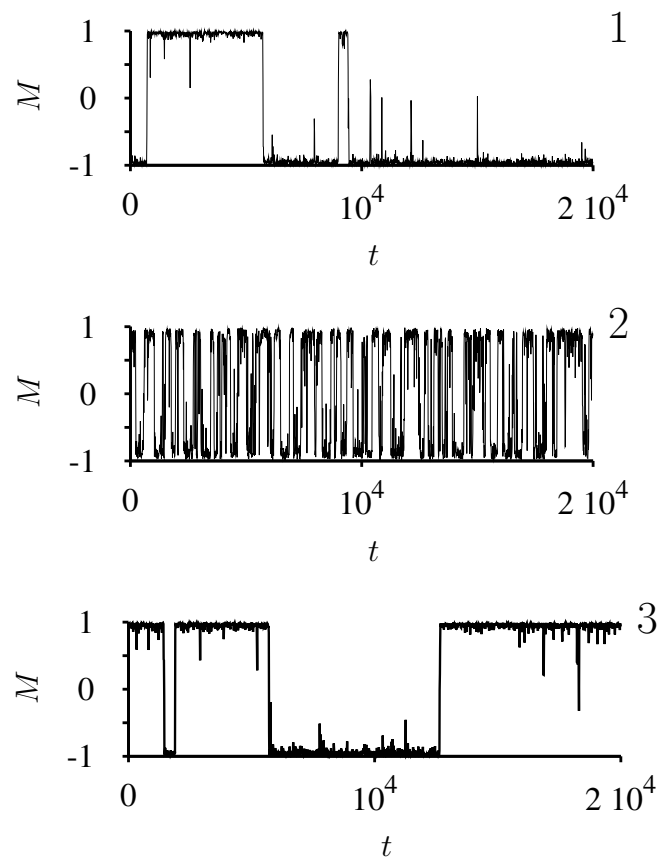


Figure 5: Evolution of  $M$  for the regime in Fig.2a with  $\psi = \cos^2 \theta$ :  $C_\psi = 2$  (1),  $C_\psi = -1$  (2) and  $C_\psi = 3$  with  $\psi = \cos^2 \theta \cos^2 \varphi$  (3).

